Energy-Autonomous Wireless Implantable Sensors powered by Piezoelectric Transducers with Magnetic Plucking

Hailing Fu[1,2], George Gibson[2], Boli Chen[3], Fang Deng[1]

1. School of Automation, Beijing Institute of Technology, Beijing 100081
E-mail: hailing.fu@bit.edu.cn and dengfang@bit.edu.cn

2. Wolfson School of Mechanical, Electrical and Manufacturing Engineering, Loughborough University, LE11 3TU, UK
E-mail: g.gibson-18@student.lboro.ac.uk

3. Department of Electronic and Electrical Engineering, University College London, WC1E 6BT, UK
E-mail: boli.chen@ucl.ac.uk

Abstract: Wireless sensors have been increasingly used in various industrial applications especially with the proliferation of the Internet of Things. In this work, an energy-autonomous solution for wireless implantable sensors is developed and illustrated, allowing medical implants to be self-sustained within the human body over long terms. This solution consists of a piezoelectric transducer with a tip magnet mounted on an implantable sensor and a wearable rotating magnetic array which can be driven either by human motion or motors. A complete theoretical model has been established in this work to study the electromechanical dynamics and the wireless power transfer capability. Different magnetic array configurations are explored to increase the power transfer distance and output level. A prototype was fabricated and tested in laboratory conditions along with a power management and control solution to verify the concept and the design. The wireless power transfer solution delivers around 0.28 mW power using a 26.5×1.5×0.3 mm piezoelectric beam, over a large transmission distance 18 mm, demonstrating its capability in implementing energy-autonomous wireless implantable sensors.

Key Words: Wireless Sensors, Internet of Things, Intelligent Systems, Wireless Power Transfer, Piezoelectric Transducers, Implantable Devices.

1 Introduction

Implantable devices have been widely used to monitor or treat chronic diseases over several decades, e.g. diabetes or heart diseases [1]. The first successful implantation of a pulse-generating cardiac pacemaker to treat Stokes-Adams syndrome was performed on Swedish patient Arne H.W. Larsson in 1958 [2]. This marked the beginning of the use of medical implants as a method of continuous intracorporeal treatment. However, how to autonomously power those implantable devices has always been a continuing challenge ~~until,~~ although many endeavors have been made [3]. Energy-autonomy can be realized ~~into~~ by two methods, including passive energy harvesting [4, 5] and active wireless power transfer [6, 7]. In 1959, Abrams et al. developed an inductive coupling charging technique [8] and Glenn et al. devised a radiofrequency transmission powering solution to address the inconvenience of carrying pacemakers and reduce the risk of infection from epicardial leads [9]. These solutions are potentially the earliest examples of wireless power transfer (WPT) in the medical industry.

Nowadays, along with the development of more functional and miniaturized medical implants, powering and maintaining medically implanted devices (MID) is crucial to healthcare infrastructure, given that medical implants offer improved diagnosis, targeted drug delivery, restoration of critical body functions, physiological data collection, and therapeutic applications [10]. Passive energy harvesting refers to the sustainable conversion of ambient energy sources into electrical power using energy harvesters, whereas WPT utilizes the energy supplied to an active transmitter to excite a receiver. Wirelessly powering these devices greatly reduces the need ~~of~~ wiring or replacing batteries along with the risk of postsurgical complications. Self-sustained implants need a continuous power supply to function effectively, especially with the additional power requirements for transcutaneous wireless communication with other medical devices outside human bodies. Various techniques have been developed in the past decade for wireless power transfer between an active transmitter and an electromechanical receiver using electromagnetic, light or acoustic waves [11, 12]. These methods allow devices that are difficult to access due to their location or environment to benefit from this indirect power connection. Energy can be transmitted through different mediums, such as skin tissue or metallic enclosures, depending on the chosen technique.

Inductive power transfer is a commonly used wireless power transfer (WPT) mechanism in biomedical implantable devices. Vennemann et al. developed a blood flowmeter powered by near field communication (NFC) using a smart phone [13], and the power can be transmitted over several millimeters. Krishnan et al. presented a skin sensor powered via NFC [14], while Yang et al. studied a similar wireless power transfer solution without a digital communication protocol [15]. Metamaterials have been extensively studied as a means of improving the efficiency of RF power transfer to medical implants. It enhances electromagnetic coupling and shielding, allowing for greater total transmitted power [16]. Pokharel et al. proposed a metamaterial-inspired WPT solution that reduces magnetic field dispersion [16], while

*This work is supported by National Natural Science Foundation (NNSF) of China under Grant 00000000.

Zhou et al. utilized metamaterials to improve efficiency and electromagnetic shielding in WPT [17].

Compared to inductive power transfer, the ultrasonic power transfer method exhibits a variety of advantages in various applications. For example, ultrasound can easily penetrate enclosed metal structures and has less attenuation in water when compared to electromagnetic waves. As the human body is composed mainly of water with dissolved electrolytes, ultrasonic power transfer can be a suitable wireless power transfer (WPT) method for medical implants. Charthad et al. successfully developed an implantable device powered by ultrasound that can transmit data through RF communication [18]. Song et al. demonstrated an omni-directional USPT system for implants, achieving 2.7% efficiency over a distance of 20 cm [19]. StimDust is an advanced solution for ultrasonic power transfer with excellent system integration [20, 21]. This solution comprises a functional neural stimulator with data uplink and downlink capabilities, with the peak electrical input-to-stimulation efficiency reported at 82%. Despite significant progress in the field of wireless power transfer for implantable devices, practical application of these solutions is still challenging due to factors such as high fabrication costs, hardware or algorithm complexity, and power transfer capability. [22, 23].

In this paper, an easy-to-implement wireless power transfer solution for energy-autonomous medical implants is studied using an implanted piezoelectric receiver with a tip magnet and a rotating wearable magnetic array. This solution offers the advantages of low operating frequency, less heat generation in tissues, and easy-to-miniaturize. The design, operating mechanism, modelling and experimental study will be introduced in the following sections.

2 Ultrasonic Power Transfer using Piezoelectric Transducers

2.1 System Design and Operating Principle

The design and operating principle of the wireless power transfer solution is illustrated in Figure 1. An implantable piezoelectric receiver with a tip magnet is capsulated and placed inside human arm to monitor critical physiological parameters. To activate the piezoelectric receiver wirelessly, a wearable rotating magnetic array is placed on human arm to provide the active power input. The magnetic coupling between the rotating magnetic array and the tip magnet on the piezoelectric beam establishes the power link between the wearable device and the implantable device. The beam is stimulated by the rotating magnets and vibrates along with the magnetic force. The number of pole pair of the array and the rotating speed determines the excitation frequency of the piezoelectric beam. In terms of the driving source of the rotating magnetic array, it can be realized by motors or directly using human motions. In this work a motor is used to provide the power source.

The intensity of the magnetic field is the key for wireless power transfer over longer distances. In order to intensify the magnetic field, the Halbach array concept is adopted with different configurations. This array adopts a specific pattern for the magnetization direction of typically four magnets as a group, and this group can be repeated in a linear or a circular way to establish multiple pole pairs, as shown

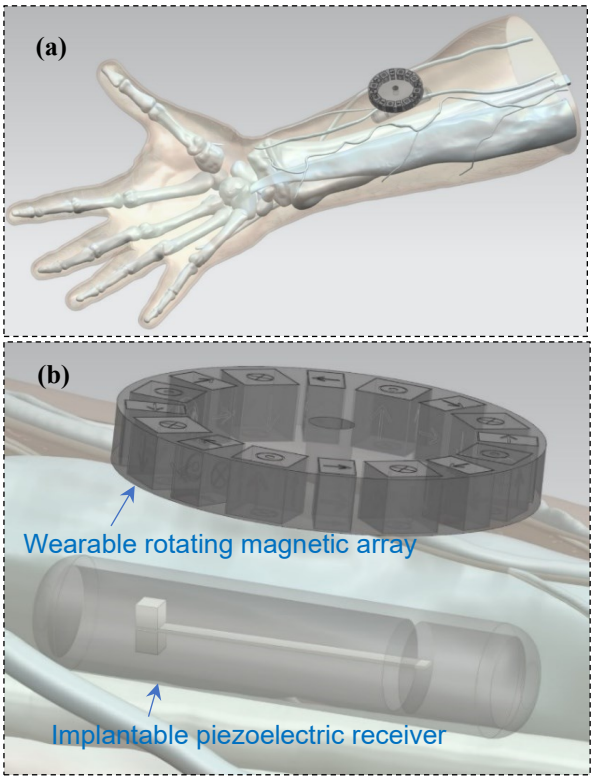

Fig. 1: Schematic diagram of the wireless power transfer solution using a piezoelectric transducer and a rotating magnetic array. (a) Solution implemented on human arm and (b) details showing the location of the implanted capsule and the wearable magnetic array.

in Figure 2(c). Such an array creates a unique feature of the magnetic field with one intensified side and one weak side. This special feature allows the magnetic field to penetrate the human tissue over a longer distance, facilitating wireless power transfer for implantable devices. Therefore, the strong

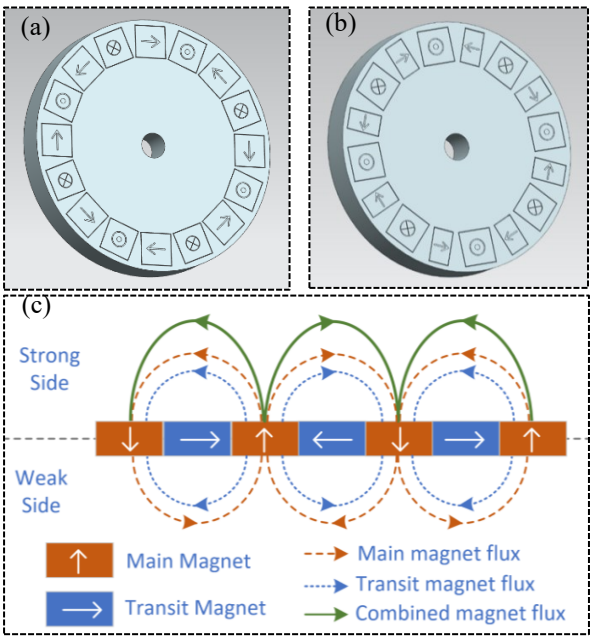

Fig. 2: Magnetic Halbach array design with different transit magnets. (a) Same dimensions for main and transit magnets and (b) smaller transit magnets and (c) Halbach array configuration and flux distribution.

side faces the implantable devices, and the weak side is typically exposed to the environments. The weak magnetic field also avoids the disturbance of the magnetic field on other wearable devices.

In order to intensify the magnetic field further within a confined space, different dimensions of the transit magnets are proposed to increase the magnetic field and pole pairs on the strong side of the magnetic field, as shown in Figure 2 (a) and (b). Smaller transit magnets allow more space to put more magnets on the rotating array. Parametric studies will be presented in the following sections to illustrate the effectiveness of different Halbach array designs.

2.2 Theoretical Modelling of Magnetic Plucking

In order to study the dynamics of the system and to examine the performance regarding wireless power transfer, a theoretical model is established, including the magnetic force model for the Halbach array and the electromechanical model for the piezoelectric transducer. Figure 3 shows the relative geometry correlation between one of the driving magnets in the Halbach array and the tip magnet on the piezoelectric receiver.

The magnetic force between the tip magnet on the implanted piezoelectric receiver and the driving magnets on the Halbach array in different magnetization directions can be determined using the following equation.

$$F_z = \frac{J_1 \cdot J_2}{4\pi\mu_0} \times \sum_{i=0}^{1}\sum_{j=0}^{1}\sum_{k=0}^{1}\sum_{l=0}^{1}\sum_{p=0}^{1}\sum_{q=0}^{1}(-1)^{i+j+k+l+p+q} \times \emptyset_z \quad (1)$$

where the function $\emptyset_z$ determines the magnetization direction and geometric information. J_1 and J_2 are the remanence value of the driving and tip magnets respectively. For the parallel magnetization direction ($+Z$ or $-Z$) the magnitude of the z component force is calculated using:

$$\emptyset_z = -U_{ij}W_{pq}ln(r-U_{ij}) - V_{kl}W_{pq}ln(r-V_{kl}) + U_{ij}V_{kl}arctan\left(\frac{U_{ij}V_{kl}}{W_{pq}r}\right) - W_{pq}r \quad (2)$$

In the case of the perpendicularly magnetized driving magnets, the function $\emptyset_z$ in Equation (1) becomes:

$$\emptyset_z = \frac{({U_{ij}}^2-{W_{pq}}^2)}{2}ln(r+V_{kl}) - U_{ij}V_{kl}ln(r-U_{ij}) - U_{ij}W_{pq}arctan\left(\frac{U_{ij}V_{kl}}{W_{pq}r}\right) - \frac{1}{2}V_{kl}r \quad (3)$$

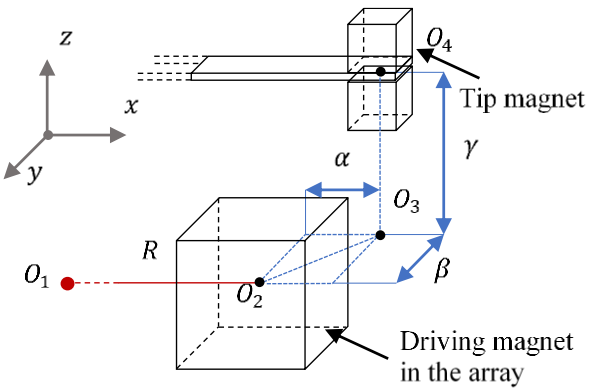

Fig. 3: Geometry relationship between one of the driving magnets on the Halbach array and the implanted piezoelectric receiver.

where U_{ij}, V_{kl} and W_{pq} are intermediary variables that define the distance between the corner points of each Halbach magnet to their respective projection on the *x*, *y* and *z* axis. These variables can be expressed as

$$\begin{cases} U_{ij} = \alpha + (-1)^j A - (-1)^i a \\ V_{kl} = \beta + (-1)^l B - (-1)^k b \\ W_{pq} = \gamma + (-1)^q C - (-1)^p c \\ r = \sqrt{{U_{ij}}^2 + {V_{kl}}^2 + {W_{pq}}^2} \end{cases} \quad (4)$$

where $2A \times 2B \times 2C$ ~~are~~ the size of the Halbach array magnets, and 2a × 2b × 2c are the dimensions of the tip magnet of the piezoelectric receiver. The gaps between two magnets in three axes are

$$\begin{cases} \alpha = R - \left(R \times \cos\left(2\pi f t_{pl} - 2\pi a\right)\right), \\ \beta = R \times \sin\left(2\pi f t_{pl} - 2\pi a\right), \\ \gamma = \left|\overrightarrow{O_3O_4}\right| + z_{disp}, \\ R = \left|\overrightarrow{O_1O_2}\right|. \end{cases} \quad (5)$$

where R is the radius of the rotating magnetic array, f is the rotating frequency, $2\pi a$ is the initial angle of each driving magnet and z_{disp} is the displacement of the beam.

2.3 Theoretical Modelling of Piezoelectric Receiver

The piezoelectric receiver performs the function of converting alternating magnetic field into electrical energy. This subsection provides the theoretical model for the piezoelectric receiver undergoes external magnetic forces. The mechanical dynamics of the piezoelectric beam can be described as

not defined

$$\frac{d^2\eta_r(t)}{dt^2} + 2\zeta_r\omega_r\frac{d\eta_r(t)}{dt} + \omega_r^2\eta_r(t) - \vartheta_r V(t) = F_m^z\phi_r(L_p) \quad (6)$$

where $\eta_r(t)$ is the modal mechanical coordinate of the beam with respect to its rth mode shape, ζ_r is the modal damping ratio, ω_r is the effective undamped modal frequency of the rth mode shape, $\phi_r(L_p)$ is the mass normalized eigenfunction at the beam tip and F_m^z is the external magnetic forces applied on the beam by driving magnets. These values can be determined by the magnetic coupling model presented in Section 2.2. The detailed process on how to obtain Eq. (6) can be found in ~~Ref.~~ [24].

The corresponding electrical equation of a piezoelectric beam connected with a resistive load R_l is

$$C_p\frac{dV(t)}{dt} + \frac{V(t)}{R_l} + \sum_{r=1}^{\infty}\vartheta_r\frac{d\eta_r(t)}{dt} = 0, \quad (7)$$

where C_p is the inherent capacitance of the piezoelectric beam. The electromechanical dynamics of the harvester can be solved using Eqs. (1)–(7).

3 Numerical Results

In this section, the theoretical model is solved numerically in MATLAB to study the dynamics of the WPT system, including magnetic forces for different dimensions and the

output voltage generated by the piezoelectric receiver under different operational conditions.

3.1 Magnetic Forces from the Array

The magnetic forces from the Halbach array are first studied, as shown in Figure 4. Figure 4(a) shows the magnetic forces from individual driving magnets on the Halbach array, since the magnets are arranged in a circular manner, the magnetic forces exhibit certain phase shifts. Magnet 1-4 in Figure 4(a) forms a complete Halbach array unit and these patents are normally repeated to form more pole pairs in the array, as shown in Figure 2(c).

Figure 4(b) shows the summation of all the forces from the Halbach array on the tip magnet. The results are very close to a sinusoidal shape and the cycles per array revolution is determined by the pole pairs. Since 16 magnets are used in this study to form a 4-pole pair array, 4 cycles are obtained in the overall magnetic force curve per array revolution. This sine-shaped magnetic force will be the external force applied on the piezoelectric beam. Therefore, the magnitude of the force is critical for wireless transfer over longer distances.

Different number and sizes of magnets, radii and transfer distance also affect the magnetic field distribution and WPT performance, as shown in Figure 5. With the increase of the magnet number, the overall force is more stabilized and closer to a sine wave with enhanced amplitude, as shown in Figure 5(a). The force increase along with the increase of the array radius since larger magnets can be fitted in the array.

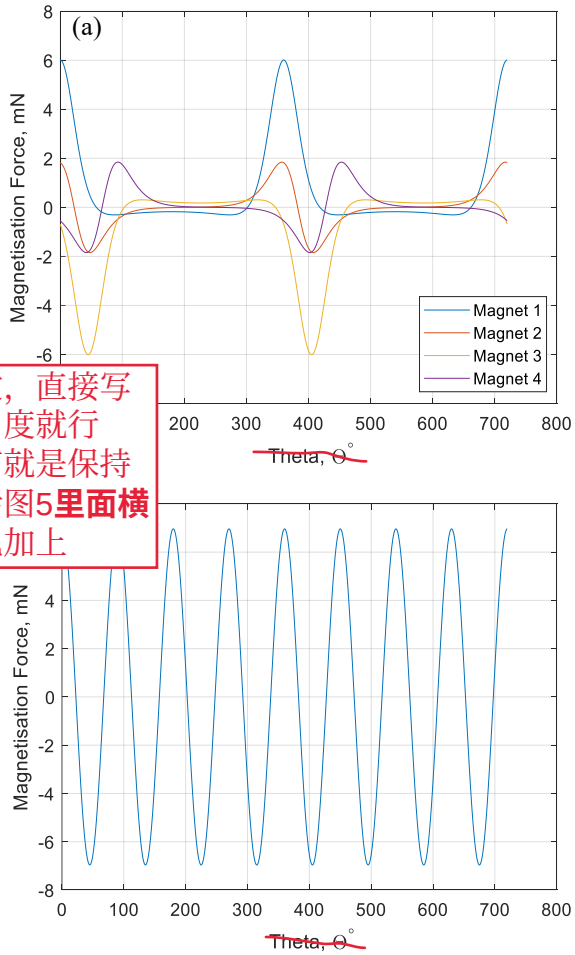

没定义过，直接写是什么角度就行了，还有就是保持一致的话图5里面横轴标签也加上

Fig. 4: Magnetic forces applied on the tip magnet from the driving magnets on the Halbach array. (a) four magnets from the array and (b) the summation of all the forces from the array over a distance, γ of 18mm.

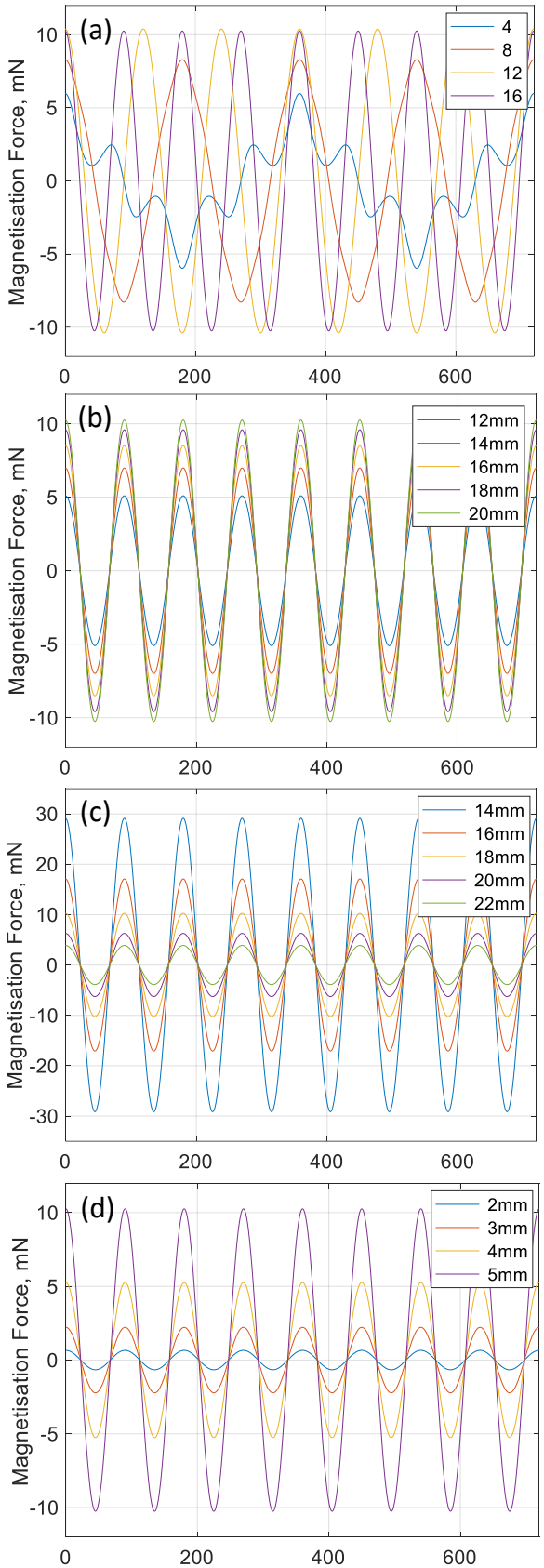

Fig. 5: Overall magnetic force variation for different design parameters: (a) number of magnets (b) Halbach array radius (c) transfer distance and (d) magnet size.

uncertainties?

See Figure 5 (b). In Figure 5(c) the force decreases when the transfer distance is longer, and the force increase again with the increase of the magnet sizes. See Figure 5(d). Therefore, there is a large freedom to optimize the system considering the constraints in size, transfer distance and frequency.

3.2 Section and Subsection Headings ?

Then the overall WPT performance is studied with the piezoelectric receiver model. The output voltage from the piezoelectric receiver is compared against magnet size and power transfer distance, as shown in Figure 6. The output voltage increases with the magnet size, but decreases sharply when the transfer distance is increased. Therefore, a trade-off between the magnet size and the transfer distance is necessary to deliver sufficient power over certain distances.

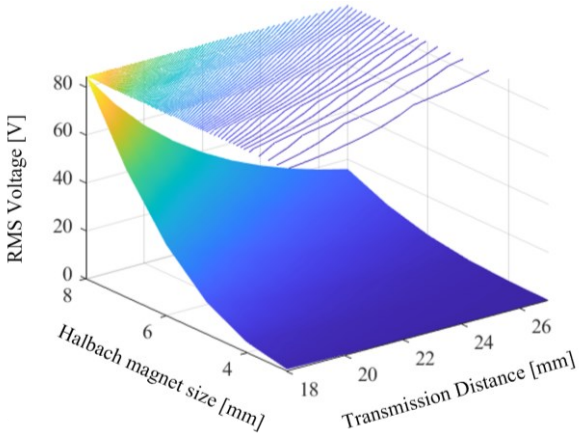

Fig. 6: Output voltage of the piezoelectric receiver against driving magnet size and power transfer distance.

4 Prototyping and Experimental Results

In order to verify the concept and validate the numerical results, a prototype was fabricated, assembled and tested in the laboratory conditions to examine the wireless power transfer capability for implantable sensors.

4.1 Prototyping and Experimental Setup

The whole experimental set-up is shown in Fig. 7(a). The Halbach array in Fig. 7(c) is mounted on a miniaturized DC motor to produce the needed rotational motion. The piezoelectric beam with a tip magnet is capsulated and mounted on a 3-axis optical stage, which can accurately adjust the gaps between the wearable transmitter and the receiver. A power management circuit LTC3588-1 is adopted to regulate the generated energy from the piezoelectric receiver. The main dimensions of the whole system are summarized in Table 1.

Table 1: Key dimensions of the WPT system

Components	Dimensions	Units
Piezoelectric beam	26.5×1.5×0.3	mm
Tip Magnet	1.5×1.5×1.5	
Halbach Array Radius	40	mm
Main magnet in Halbach Array	4×4×4	mm
Transfer Distance	>10	mm

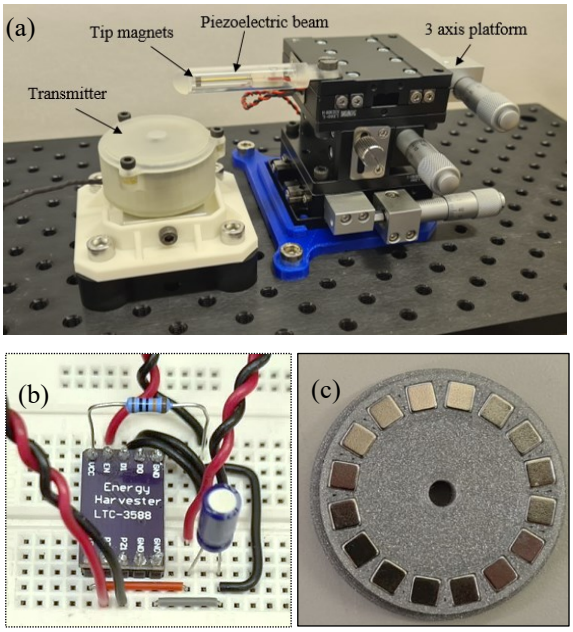

Fig. 7: WPT prototype and experimental set-up. (a) Whole set-up; (b) power management circuit and (c) Halbach array.

4.2 Experimental Results

The WPT solution is tested under different transfer distance with different magnet sizes, as shown in Fig 8. Larger magnets can obtain higher output voltages as expected, and the output voltage reduces as the transfer distance increases. The system can generate more than 6 volts at the distance of 20 mm. Another effect examined is the strong and weak sides of Halbach arrays. Compared to the weak side, much higher output voltage is obtained from the strong side at the same distance.

The power transfer capability is further examined with a power management circuit, LTC3588-1, which can rectify the alternating-current output into the direct-current form at a desired range stored in a storage capacitor. Whilst the discharge resistor of 100kΩ was kept constant, three electrolytic capacitors of values 1μF, 22μF and 1mF were tested to see the effect on the charging time. As expected, using a larger capacitor resulted in longer charging and discharging time periods (τ_c and τ_d) but yielded a greater storage of the transferred energy. The system takes approximately 6.2 seconds to charge and 2.6 seconds to

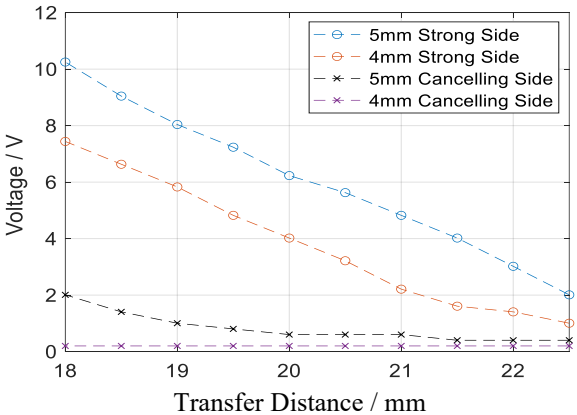

Fig. 8: Output voltage of the piezoelectric receiver for different transfer distances for the strong side and weak side of the Halbach array.

discharge, resulting in useable power output of ~10 µW for a 22µF capacitor.

5 Conclusion and Future Work

A method of electrodynamic wireless power transfer has been developed as a battery-free sensing solution for medical implants. A rotating Halbach array has been used as the contactless near-field transmitter with a piezoelectric receiver to establish the wireless power link. A theoretical model was established to study WPT dynamics, including the magnetic force interactions between the transmitting and receiving magnets and the electromechanical dynamics of the piezoelectric receiver. A prototype was developed and tested along with a power management circuit. 88.9µJ of energy can be stored within a 22µF capacitor in a 6.2 second charging cycle, which means an average output power of 10.1µW was obtained using this WPT method, providing a feasible solution to power implantable devices. Future directions include device miniaturization, sensing function integration and device bio-compatibility.

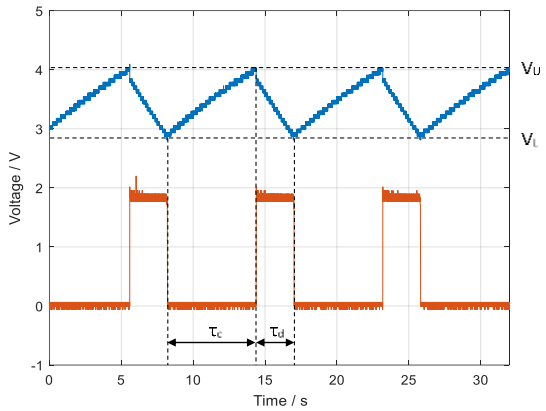

Fig. 9: WPT charging and discharging cycles using a power management circuit with a storage capacitor.

References

[1] T. He and C. Lee, "Evolving flexible sensors, wearable and implantable technologies towards BodyNET for advanced healthcare and reinforced life quality," IEEE Open Journal of Circuits and Systems, vol. 2, pp. 702-720, 2021.

[2] B. Larsson, H. Elmqvist, L. Ryden, and H. Schüller, "Lessons from the first patient with an implanted pacemaker: 1958–2001," Pacing and Clinical Electrophysiology, vol. 26, no. 1p1, pp. 114-124, 2003.

[3] M. J. Karimi, A. Schmid, and C. Dehollain, "Wireless power and data transmission for implanted devices via inductive links: A systematic review," IEEE Sensors Journal, vol. 21, no. 6, pp. 7145-7161, 2021.

[4] H. Fu, J. Jiang, S. Hu, J. Rao, and S. Theodossiades, "A multi-stable ultra-low frequency energy harvester using a nonlinear pendulum and piezoelectric transduction for self-powered sensing," Mechanical Systems and Signal Processing, vol. 189, p. 110034, 2023.

[5] H. Fu et al., "Rotational energy harvesting for self-powered sensing," Joule, vol. 5, no. 5, pp. 1074-1118, 2021.

[6] Z. Zhang, H. Pang, A. Georgiadis, and C. Cecati, "Wireless power transfer—An overview," IEEE Transactions on Industrial Electronics, vol. 66, no. 2, pp. 1044-1058, 2018.

[7] M. Song et al., "Wireless power transfer based on novel physical concepts," Nature Electronics, vol. 4, no. 10, pp. 707-716, 2021.

[8] L. Abrams, W. Hudson, and R. Lightwood, "A surgical approach to the management of heart-block using an inductive coupled artificial cardiac pacemaker," The Lancet, vol. 275, no. 7139, pp. 1372-1374, 1960.

[9] W. W. Glenn, A. Mauro, E. Longo, P. H. Lavietes, and F. J. Mackay, "Remote Stimulation of the Heart by Radiofrequency Transmission: Clinical Application to a Patient with Stokes–Adams Syndrome," New England Journal of Medicine, vol. 261, no. 19, pp. 948-951, 1959.

[10] S. Chatterjee, M. Saxena, D. Padmanabhan, M. Jayachandra, and H. J. Pandya, "Futuristic medical implants using bioresorbable materials and devices," Biosensors and Bioelectronics, vol. 142, p. 111489, 2019.

[11] F. Erkmen and O. M. Ramahi, "A scalable, dual-polarized absorber surface for electromagnetic energy harvesting and wireless power transfer," IEEE Transactions on Microwave Theory and Techniques, vol. 69, no. 9, pp. 4021-4028, 2021.

[12] H. Fu, J. Rao, M. S. Harb, and S. Theodossiades, "Ultrasonic wireless power links for battery-free condition monitoring in metallic enclosures," Ultrasonics, vol. 114, p. 106395, 2021.

[13] B. Vennemann, D. Obrist, and T. Rösgen, "A smartphone-enabled wireless and batteryless implantable blood flow sensor for remote monitoring of prosthetic heart valve function," PLoS One, vol. 15, no. 1, p. e0227372, 2020.

[14] S. R. Krishnan et al., "Wireless, battery - free epidermal electronics for continuous, quantitative, multimodal thermal characterization of skin," Small, vol. 14, no. 47, p. 1803192, 2018.

[15] S. Yang et al., " “Cut - and - paste” manufacture of multiparametric epidermal sensor systems," Advanced Materials, vol. 27, no. 41, pp. 6423-6430, 2015.

[16] R. K. Pokharel, A. Barakat, S. Alshhawy, K. Yoshitomi, and C. Sarris, "Wireless power transfer system rigid to tissue characteristics using metamaterial inspired geometry for biomedical implant applications," Scientific reports, vol. 11, no. 1, p. 5868, 2021.

[17] J. Zhou, P. Zhang, J. Han, L. Li, and Y. Huang, "Metamaterials and metasurfaces for wireless power transfer and energy harvesting," Proceedings of the IEEE, vol. 110, no. 1, pp. 31-55, 2021.

[18] J. Charthad, M. J. Weber, T. C. Chang, M. Saadat, and A. Arbabian, "A mm-sized implantable device with ultrasonic energy transfer and RF data uplink for high-power applications," in Proceedings of the IEEE 2014 Custom Integrated Circuits Conference, 2014: IEEE, pp. 1-4.

[19] S. H. Song, A. Kim, and B. Ziaie, "Omnidirectional ultrasonic powering for millimeter-scale implantable devices," IEEE Transactions on Biomedical Engineering, vol. 62, no. 11, pp. 2717-2723, 2015.

[20] D. K. Piech et al., "A wireless millimetre-scale implantable neural stimulator with ultrasonically powered bidirectional communication," Nature biomedical engineering, vol. 4, no. 2, pp. 207-222, 2020.

[21] D. K. Piech et al., "StimDust: A mm-scale implantable wireless precision neural stimulator with ultrasonic power and communication," arXiv preprint arXiv:1807.07590, 2018.

[22] G. L. Barbruni, P. M. Ros, D. Demarchi, S. Carrara, and D. Ghezzi, "Miniaturised wireless power transfer systems for neurostimulation: A review," IEEE Transactions on Biomedical Circuits and Systems, vol. 14, no. 6, pp. 1160-1178, 2020.

[23] N. Nguyen, N. Ha-Van, and C. Seo, "Midfield wireless power transfer for deep-tissue biomedical implants," IEEE Antennas and Wireless Propagation Letters, vol. 19, no. 12, pp. 2270-2274, 2020.

[24] A. Erturk and D. J. Inman, "An experimentally validated bimorph cantilever model for piezoelectric energy harvesting from base excitations," Smart materials and structures, vol. 18, no. 2, p. 025009, 2009.